Computer Communications 000 (2015) 1–14

Contents lists available at ScienceDirect

Computer Communications

journal homepage: www.elsevier.com/locate/comcom

On configuring radio resources in virtualized fractional frequency reuse cellular networks

Xin Wang*, Prashant Krishnamurthy, David Tipper

School of Information Sciences, University of Pittsburgh, Pittsburgh, PA 15260, United States

ARTICLE INFO

Article history:
Received 17 October 2014
Revised 2 September 2015
Accepted 31 October 2015
Available online xxx

Keywords:
Wireless network virtualization
Service provider
Radio resources configuration
Fractional frequency reuse

ABSTRACT

Virtualization of wireless networks holds the promise of major gains in resource usage efficiency through spectrum/radio resources sharing. Unlike the case in wired networks, achieving high capacity, providing effective isolation, and customization of the network requires intelligent configuration of wireless resources due to the effects of interference. In this paper, we focus on how to configure the "over-the-air" part of virtual wireless networks to enable simultaneous use of radio resources that overlap geographically. A configuration framework is proposed based on an infrastructure cellular network that employs fractional frequency reuse (FFR) and Multiple-input Multiple-output (MIMO) to combat interference. Multiple scenarios are examined that include various network sizes and base station distances. Five radio resources configuration cases are developed and investigated with each of these scenarios for a number of parameter settings (e.g., transmit power, MIMO degree). From the analysis of capacity data obtained from simulations, we observe some general trends in the aggregate spectral efficiency, and more importantly, a variety of tradeoffs between service providers (SPs) or virtual network operators. Based on these tradeoffs, we create configuration maps using which, a network resource manager can select specific network configurations (transmit power, MIMO, etc.) to meet the demand and capabilities of SPs and their subscribers.

1. Introduction

The explosive capacity demand in cellular networks has required network operators to increase capital (CAPEX) and operational expenses (OPEX) in order to improve their networks accordingly. However, operators have to control cost due to the predicted decreasing profit margin [1]. Therefore, *wireless network virtualization* has been proposed recently, with the benefits of increasing resource efficiency, enabling customized applications, and yet providing isolation between services [2]. The premise here is that spectrum, hardware, and network resources in wireless networks can be sliced on demand in a manner similar to CPU, storage, and memory in data center virtualization or network bandwidth in wired network virtualization to support customized services. To facilitate this virtualization, the functions of traditional network operators are expected to be split into two entities – Infrastructure providers (InPs) and Service Providers (SPs). InPs own the spectrum, hardware, and network resources. The "users" are SPs who get slices of these resources dynamically to support the services they provide to their own subscribers [2]. A *resource manager* is responsible for providing the correct configuration of resource slices for various SPs in each time period (see Fig. 1(a)). Spectrum aggregation or pooling [3] is considered as a major feature (pooling together each InP's spectrum for configuration by the resource manager and assignment to SPs) with the potential for large gains in spectrum efficiency.

Wireless network virtualization is a solution that breaks down the old fixed network architecture towards better efficiency, customization, and isolation. Implementing it on an existing physical network implies that we need not physically tear down the existing one and build up a brand new one. Instead, we just remove the "fixed" way of using resources and add a new management entity to dynamically realize multiple architectures on existing physical resources. A core problem is how we should manage the "virtual" resources. Previous work [4,5] on wireless network virtualization assumes "separate spectrum virtualization" (SSV), where spectrum is sliced, but in a completely *separate* or *orthogonal* manner for SPs in any given time period. As shown in the top half of Fig. 2, the spectrum slices allocated to SP_A, SP_B, and SP_C in the same time interval do not overlap, but may change dynamically in time.

However, spectrum is not like CPU resources or wired network bandwidth. Transmit powers, interference, mobility, channel conditions, the use of MIMO (device capability), distances between transceivers, all impact the available *capacity*. To exploit spectrum pooling , the work in [6] introduces "radio resource virtualization" (RRV) that allows a certain overlapping allocation of the spectrum

* Corresponding author. Tel.: +1 412 624 5144; fax: +1 412 624 2788.
E-mail address: xiw54@pitt.edu, julywang.cn@gmail.com (X. Wang).

http://dx.doi.org/10.1016/j.comcom.2015.10.013
0140-3664/

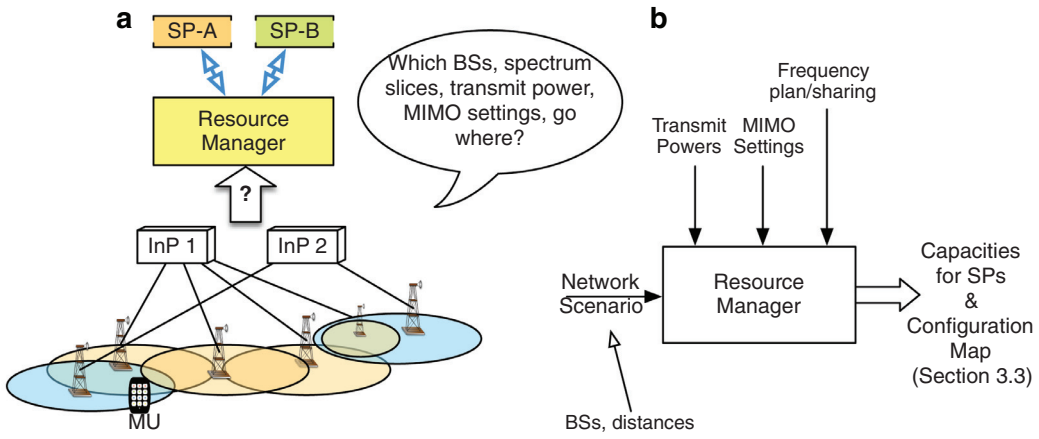

Fig. 1. High level view of wireless network virtualization considered in this paper.

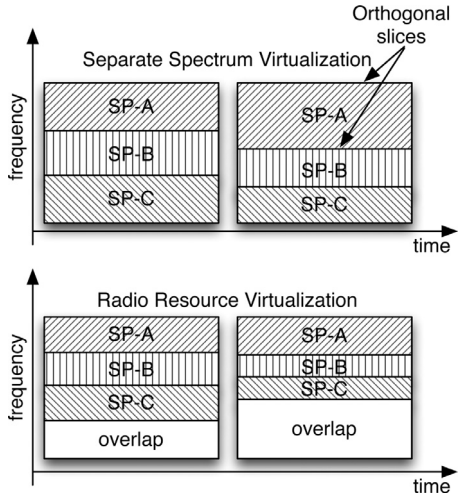

Fig. 2. Separate spectrum virtualization (SSV) vs. radio resource virtualization (RRV).

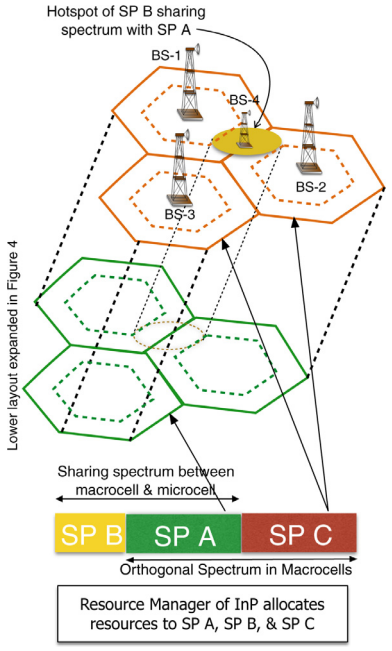

Fig. 3. A multicell virtual system with FFR. (For interpretation of the references to color in this figure legend, the reader is referred to the web version of this article.)

slices to multiple SPs in the same time interval in neighboring or even overlapping geographic coverage areas. As shown in the lower half of Fig. 2, the "overlap" slices could be used by all three SPs with careful planning. In fact, the work in [6] illustrates (albeit in a simple scenario) why spectrum should be considered as a "radio resource" and that RRV often leads to better resource efficiencies compared to SSV [1].

The core problem therefore turns into how we manage cellular networks considering RRV. One question to ask is how can we configure the network to enable RRV to achieve the best resource utilization? Unfortunately, there is no definite or simple answer yet. The configuration problem becomes even more complicated as the network architecture becomes more complicated, such as when frequency reuse is adopted. For example, the resource manager has to decide what power level (in a given slice of spectrum) should be assigned to a given SP in a given cell. It has to determine how many antennas a given SP (or mobile units (MUs)) can use in a given cell. It has to decide how these may change depending on the distances between infrastructure entities such as base stations (BSs)). One example of the results of this paper shows that SPs that are deployed in smaller cells can benefit significantly by using the spectrum of SPs that are deployed over larger cells. However, if such configurations are enabled, the capacity of SPs deployed in larger cells may drop by 20% per subscriber. If the demand in larger cells can tolerate this drop (example during low load periods), this may be a preferred option for the resource manager. If not, more antennas may be used in larger cells to counteract the drop in capacity if the BS and subscriber devices are thus capable.

In this paper, we try to start answering the above questions through a framework examining several scenarios that includes a range of configuration cases. The framework constructs a cellular network with radio resources being shared between two SPs. One SP is deployed in 3 large cells with fractional frequency reuse (FFR) in these cells. The other SP operates in a smaller cell which is a subset of one of the 3 large cells. In practice, it is likely that many SPs may operate in many different sized cells. For example, the three-SP schematic (in Figs. 2 and 3) illustrates the generalized sharing problem. In such

[1] Please note that in this paper, from now unless otherwise specified, we use the word "spectrum" to mean radio resources.

scenarios, simultaneous usage of spectrum across SPs can be possibly limited in many spectrum slices or in small areas near BSs. Most SPs would be configured to use dedicated/orthogonal slices of spectrum for the rest of their coverage. Our focus is on the more complex problem of SPs that may be configured to use the "overlapping" slices of spectrum (see the low half of Fig. 2). We consider Multiple-input Multiple-output (MIMO) based communication systems to understand how system capacity may change with the capabilities of SPs and their subscribers.

The contribution of our work can be viewed from two aspects. From a technical perspective, we propose a framework that investigates RRV and evaluates the resource efficiency, and potentially the ability of customization and isolation in a virtual wireless network. This framework can be seen as a manual or guideline showing possible network configurations of SPs' for a resource manager. Note that the pricing of radio resources that may be dynamically leased by an SP from an InP, the cost of reconfiguration and management of the network, and service agreements between SPs and InPs, hinge on the ability to manage the radio resources appropriately. Hence, our technical evaluation of scenarios can assist in such economics and policy decisions. Tradeoffs and corresponding configurations from our investigation would be integral to a global economic optimization problem of virtualization.

The rest of this paper is organized as follow. The multi-cell system model and evaluation metrics are explained in Section 2. Section 3 presents simulation results. Limitations and extended issues are discussed in Section 4. Section 5 goes over some related work. Finally, this paper is concluded in the sixth section.

2. System models

In this section, we describe the scope of the problem, illustrate the heterogeneous system layouts and integration with RRV then explain the model used in this paper for evaluation.

2.1. Scope of the problem

Here we consider the scope of the problem at a high level. The details are provided in subsequent sub-sections.

Consider a cellular network that consists of multiple BSs, of which four are shown in the shown in Fig. 3 (BS-1 to BS-4). The BSs can be configured for use by multiple SPs (they are part of the "hard metal" infrastructure being shared by virtual networks). The usage may generally vary – in Fig. 3, we show two SPs, namely, SP_A and SP_C making use of BS-1, BS-2, and BS-3 at the same time, each having the same approximate coverage. The spectrum used by SP_A and SP_C are orthogonal (in a manner similar to SSV). We assume that the slicing of resources between them is completely orthogonal with minimal interaction between them.

In contrast, SP_A and SP_B are configured such that they are sharing spectrum (see bottom of Fig. 3 and described below in more detail). The spectrum in green would have been configured for use by SP_A only with SSV and the spectrum in yellow would have been configured for use by only SP_B. In the sharing configuration with RRV, the green and yellow spectra can both be used by SP_A and SP_B, but for SP_B, such a sharing occurs only in the coverage area of BS-4. In other words, we can view SP_B as operating a hotspot that is configured to use SP_A's spectrum in addition to its own. If SP_B is also using BS-1 to BS-3, SP_B is configured to use orthogonal spectrum as with SSV. The scenario we are considering here is one where SP_A and SP_B are configured such that the *spectrum that is shared, is used over the three macro-cells served by BS-1 to BS-3 for subscribers of* SP_A, *and one micro-cell served by BS-4 for subscribers of* SP_B. If spectrum is shared between the macrocells simultaneously in space and time, it is likely that the interference will be too high as we see later. Our objective is to examine the ramifications of this sharing that is somewhat limited in space. Shannon channel capacities (introduced in Section 2.3) are evaluated to measure the benefit of sharing. As capacity provided by a certain chunk of spectrum depends on various factors, we select a set of influential parameters (BS transmit power, frequency configuration/planning (FFR) and MIMO settings) as the changeable network configuration parameters. Such configurations have different effects in the capacities that SPs can provide to their subscribers across different network scenarios. Using our framework, proper configurations can be selected to meet the requirements of various virtual players. The general idea of the framework is shown in Fig. 1(b) where the inputs to the resource manager and outputs are shown. Outside the scope of the paper is the optimization that the resource manager may have to run to satisfy the service agreements of the SPs with the InPs.

We make the following assumptions to simplify the problem:

- Dynamic orthogonal spectrum allocation/SSV (see Fig. 2) is assumed to automatically occur with our spectrum sharing scheme. As the multiplexing gain induced by SSV has been widely studied and demonstrated elsewhere [4,5,7], we do not include it in our simulations. Improvement in spectrum efficiency exclusively from RRV that is independent from multiplexing gain is the focus.
- We utilize a Shannon channel capacity upper-bound estimate of the real channel throughput and ignore communication procedures like coding, modulation, scheduling, etc. This approach, while simplified because it excludes the communications procedures, allows the framework to include influential factors like transmit power, spectrum reuse scheme, and MIMO in deciding configurations.
- In a completely virtualized system, the resource manager often makes configuration decisions every given unit of time and the configurations will change dynamically to meet the needs of the SPs. In our study, we assume the "scenario" where the resource manager sees a snapshot of the virtual network, and the suggested configuration is for that time unit. The time-scale (what should the unit be?) and the corresponding complexity in adjusting hardware are out of the scope of our work and left for future study.

We note that the above assumptions are not absolutely necessary, but we make them to simplify the problem and obtain some preliminary insights. Relaxing these assumptions would make the problem more intricate, and the number of parameters and corresponding results harder to easily visualize and generalize.

2.2. Fractional frequency reuse and radio resource virtualization cases

Expanding on the discussion, we consider a geographical area where the two SPs: SP_A and SP_B co-exist (gray area shown in Fig. 4). The resource manager configures InPs to deploy FFR in BS-1, BS-2, and BS-3 in support of SP_A. We will refer to this as SP_A's layout, where the center of three cells utilize the same frequency band f_0, and the other frequency bands are divided equally into three parts: f_1, f_2 and f_3, that are then distributed to the edges of cells 1, 2 and 3 orthogonally. We assume that BS-4 is located along the dashed line in Fig. 4 and we call this SP_B's layout in the system. Parameters d, r_A, and r_B indicate the distance between BS-4 and BS-2, the radius of cells created by BS-1, BS-2, BS-3 and the radius of the cell created by BS-4, respectively.

Note that the cells in Figs. 3 and 4 are only schematics. In reality, the cells are not hexagonal or circular in shape. The way in which we associate a MU with a BS in our simulations is as follows. In SP_A's layout, MUs are uniformly distributed within the gray area in Fig. 4, and the received signal strength (RSS) values from the three macrocells are determined for every MU. The BS that a MU should be attached to is based on the largest RSS. If the MU receives a signal with RSS smaller than a minimum received signal power, it is not attached to any of the three base stations. A minimum received signal power

Please cite this article as: X. Wang et al., On configuring radio resources in virtualized fractional frequency reuse cellular networks, Computer Communications (2015), http://dx.doi.org/10.1016/j.comcom.2015.10.013

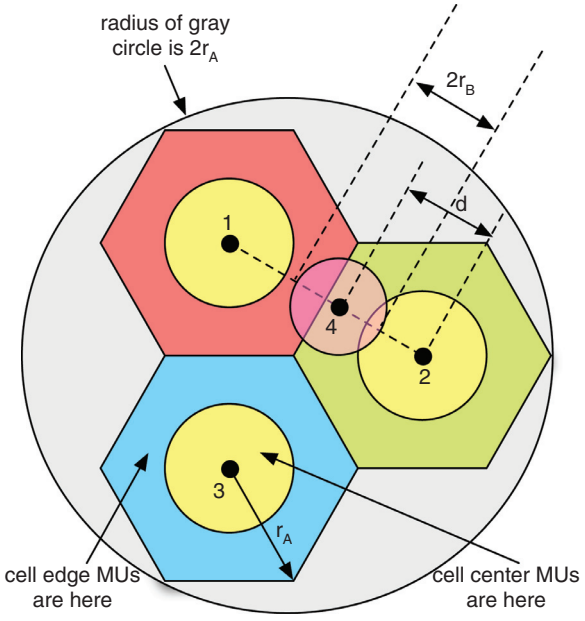

Fig. 4. 2D-schematic of multicell virtual system with FFR. (For interpretation of the references to color in this figure legend, the reader is referred to the web version of this article.)

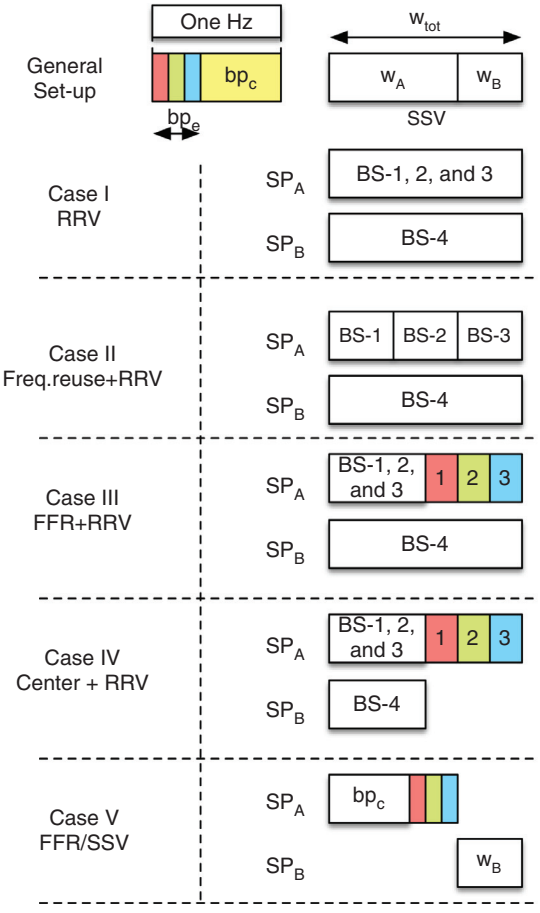

Fig. 5. Radio resource allocation cases.

threshold P_{th_A} is set by the operators depending on the equipment deployed and target data rates. If a MU's RSS (including path loss and shadow fading factor) is larger than Pr_{th_A} but smaller than $2Pr_{th_A}$ (3 dB larger than threshold), we call it a cell edge MU[2]. Otherwise, it is an MU in the center of the cell (cell-center MU). In SP_B's layout, MUs are uniformly distributed in the small cell. We make no comparison of received powers and assume all MUs subscribed to SP_B associate with BS-4. BS-4 has no separation into cell center and cell edge – that is, it does not employ fractional reuse.

Fig. 5 shows several possibilities that a resource manager can consider for configuring spectrum among the BSs for the two SPs. Suppose that w_A Hz of spectrum is allocated to the SP_A's layout and w_B Hz to the SP_B layout in the case of orthogonal spectrum allocation or SSV. This is shown at the top of Fig. 5 as two rectangles – please note that SSV is also evaluated in Section 3 along with various cases of RRV described next.

The total bandwidth available for configuration under RRV by the resource manager is $w_{tot} = w_A + w_B$. When FFR is used by SP_A, in SP_A's layout, a proportion bp_c of bandwidth is utilized by the center area of all cells (colored yellow) while the rest of the bandwidth (a proportion bp_e) is equally divided into 3 chunks (colored blue, green, and red), each of which is allocated to one cell edge (as shown in Fig. 4), such that $bp_c + bp_e = 1$ [3]. This high level view is shown as the general set up at the top of Fig. 5. We now describe the five cases (listed below the general setup in Fig. 5) that are investigated in our simulations in Section 3.

- *Case I – RRV:* In this case, there is no spectrum planning in SP_A's layout. The system is configured such that MUs can access the entire w_{tot} Hz spectrum in a time unit in all of the four cells served by BS's 1–4. Note that this has the highest potential for interference.
- *Case II – Freq. reuse + RRV:* The cells (BSs 1–3) in SP_A's layout are configured to use $\frac{1}{3}w_{tot}$ each orthogonally (traditional frequency reuse with a reuse factor of 3). No FFR is applied (i.e., the spectrum allocated to a BS is used throughout the cell). The cell of BS-4 in SP_B's layout is configured to use all of the spectra (w_{tot}) in a time unit.
- *Case III – RRV + FFR:* As described above, the center area of any cell in SP_A's layout is configured such that center MUs can access $bp_c w_{tot}$ of the bandwidth and the amount of frequency bandwidth used by cell edge MUs is $\frac{1}{3}bp_e w_{tot}$. SP_B's layout is configured such that its MUs can access the entire w_{tot} Hz spectrum in a time unit.
- *Case IV – Center + FFR + RRV:* The cells in SP_A's layout use FFR as in Case III. The center area of any cell in SP_A's layout is configured such that center MUs can access $bp_c w_{tot}$ of the bandwidth and the amount of frequency bandwidth used by cell edge MUs is $\frac{1}{3}bp_e w_{tot}$. SP_B's layout is configured such that its MUs can access, in a time unit, **only** the portion $b_{pc} w_{tot}$ Hz spectrum used by the center areas in each cell in SP_A's layout. This is unlike Case III, where all of w_{tot} could be used by BS-4. We abbreviate this as Center+RRV in the figures.
- *Case V – FFR / SSV:* This configuration corresponds to separate spectrum virtualization – it ensures that there is no sharing between the two SPs. SP_A is configured to use FFR with its own spectrum to protect cell edge MUs from severe interference. This case has the lowest potential for interference. In practice, the

[2] The cell edge number is considered as part of the FFR configuration and is changed later in simulations.

[3] We assume for simplicity in each case that each SP manages frequency bands in frequency division multiplexing (FDM) fashion for its MUs. In other words, there is no intra-cell interference (like LTE). Thus, with FFR, the available bandwidths for each of SP_A's center MU and edge MU are $bp_c w_{tot}/(nu_{Ac_k})$ and $\frac{1}{3}bp_e w_{tot}/(nu_{Ae_k})$, respectively. The available bandwidth for each of SP_B's MU is $w_{tot}/(nu_B)$. The numbers nu_{Ac_k}, nu_{Ae_k} and nu_B are numbers of the users in the center area of Cell k, edge area of Cell k and SP_B's layout, respectively. Note that $nu_{A_k} = nu_{Ac_k} + nu_{Ae_k}$ and $nu_A = \sum_k nu_{Ac_k} + \sum_k nu_{Ae_k}$. In reality, the bandwidth allocation to individual users will be more complex (e.g., physical resource blocks in LTE-like systems).

Table 1
Available frequency bandwidth per MU.

Spectrum scheme	SP_A center	SP_A edge	SP_B
Case I: RRV	$\frac{w_{tot}}{nu_{A_k}}$	$\frac{w_{tot}}{nu_{A_k}}$	$\frac{w_{tot}}{nu_B}$
Case II: Freq. reuse + RRV	$\frac{1}{3}\frac{w_{tot}}{nu_{A_k}}$	$\frac{1}{3}\frac{w_{tot}}{nu_{A_k}}$	$\frac{w_{tot}}{nu_B}$
Case III: RRV + FFR	$\frac{b_{pc}w_{tot}}{nu_{Ac_k}}$	$\frac{1}{3}\frac{b_{pe}w_{tot}}{nu_{Ae_k}}$	$\frac{w_{tot}}{nu_B}$
Case IV: Center + FFR +RRV	$\frac{b_{pc}w_{tot}}{nu_{Ac_k}}$	$\frac{1}{3}\frac{b_{pe}w_{tot}}{nu_{Ae_k}}$	$\frac{b_{pc}w_{tot}}{nu_B}$
Case V: FFR/SV	$\frac{b_{pc}w_A}{nu_{Ac_k}}$	$\frac{1}{3}\frac{b_{pe}w_A}{nu_{Ae_k}}$	$\frac{w_B}{nu_B}$

boundary between w_A and w_B changes over time, but we keep it fixed in our simulations.

One can observe from Fig. 5 that the sharing of radio resources can have intricate configurations. Immediately, it is not obvious as to which configuration will be suitable and under what circumstances. Clearly, the interference is maximum in Case I and minimum in Case V. We define nu_A as the total number of SP_A MUs and nu_B as the number of SP_B MUs. The average amount of available bandwidth per MU for SP_A is w_{tot}/nu_A if frequency bands are universally reused in the SP_A layout (Case I). In this case, many concurrent transmissions will cause excessive interference and degrade system performance. For each case, the average amount of available bandwidth for each MU (SP_A's center MU, edge MU and SP_B's MU) is summarized in Table 1. With traditional frequency reuse (Case II), frequency bands are divided equally according to a reuse factor (into 3 cells in our model resulting in a $\frac{1}{3}w_{tot}$ bandwidth per cell). This reduces interference between the cells in SP_A's layout, but reduces the capacity as well. With FFR (Case III), the amounts of available bandwidth for each "center MU" and "edge MU" are $\frac{b_{pc}w_{tot}}{nu_{Ac_k}}$ and $\frac{1}{3}\frac{b_{pe}w_{tot}}{nu_{Ae_k}}$ respectively, where nu_{Ac_k} refers number of center MUs and nu_{Ae_k} denotes the number of edge MUs in Cell k. In Case IV, only the spectrum deployed in the center area of the cells served by BSs 1, 2, and 3 in SP_A's layout is shared with SP_B reducing the amount of bandwidth that each MU in SP_B's layout gets to $\frac{b_{pc}w_{tot}}{nu_B}$ Hz. However, the interference to SP_A's cell edge MUs reduces. Case V does not allow simultaneous usage of spectrum between SPs, so MUs only access their own SP's spectrum reducing interference but also the amount of bandwidth available. FFR partition dominates the spectrum allocation in SP_A's layout (influential FFR parameters will be discussed later). It is not easy to conclude as to which configuration is generally preferable, and under what circumstances, because the achievable data rate per MU depends on how much of the radio resources is shared, the interference level, as well as factors b_{pc}, b_{pe}, nu_{Ac_k}, and nu_{Ae_k}. We further note that the range of cell edge affects the values of nu_{Ac_k} and nu_{Ae_k}.

2.3. Capacity metric

In the most general case, SP_A and SP_B may be using very different radio access technologies and devices. In order to get some insight into the potential of system capacity gains, we utilize capacity calculations rather than specific modulation, coding, and application requirements in this paper. Our objective is to consider these specific aspects in future work to the extent possible. Here, we assume that both the downlink transmissions (by all BSs for both SP_A and SP_B) employ MIMO[4] for exploring spatial degrees of freedom and for combatting any interference. We assume the commonly employed frequency-flat quasi-static MIMO fading environment, where the transmission between the ith transmit antenna and the jth receiving antenna can be modeled by

$$y = \sqrt{D^{-\alpha}10^{\zeta_j/10}}h_{ij} \times x + N \tag{1}$$

where x, y are transmit and receive signals respectively, D is the distance from a transmitter to a receiver (the transmitters are the BSs in Fig. 4, but transmissions may end up at receivers that do not belong to them as interference), α is the path loss exponent, $\zeta = N(0,\sigma)$ is the shadow fading component, h_{ij} is the Rayleigh fading channel gain of the channel between the ith transmit antenna and the jth receiving antenna, and N is the thermal noise with variance $N_0/2$. This model applies for all BSs and all SPs.

Assume that the transmission operates in a $n_T \times n_R$ downlink MIMO channel, where n_T is the number of transmit antennas at BS and n_R is the number of receiving antennas at the MU. The achievable data rate of a single MU can be estimated by the (Shannon) capacity formula [8,9],

$$C = w\log_2 \det[(\mathbf{I}_{n_R} + (\mathbf{R}^{-1/2}\mathbf{H})P_T(\mathbf{R}^{-1/2}\mathbf{H})^H] \tag{2}$$

where w is the available bandwidth for one particular MU, and the transmit power is P_T. $\mathbf{H}$ is the complex channel gain matrix, consisting of $\sqrt{D^{-\alpha}10^{\zeta/10}}h_{ij}$ where ζ varies independently for each user (but it is kept fixed over time once the sample has been drawn from the distribution for a given user). $\mathbf{R}$ is the interference and thermal noise combined matrix, which is given as:

$$\mathbf{R} = \sum_k \mathbf{H}_{Ik}\mathbf{H}_{Ik}^H P_{Ik} + wN_0\mathbf{I}_{n_R} \tag{3}$$

where $\mathbf{H}_{Ik}$ is the interfering channel matrix from interfering Cell k. For example, MUs in SP_A's layout face interference from BS-4 in the small cell but MUs in SP_B's layout receive interference from BSs 1, 2 and 3. P_{Ik} is the interferer's transmit power and $\mathbf{I}_{n_R}$ is an identity matrix **of dimensions**. From an information theoretic point of view, the capacity in Eq. (2) is equivalent to the capacity of the combined SINR channel $\mathbf{R}^{-1/2}\mathbf{H}$ under Gaussian white noise. With this interpretation, the capacity can be calculated as a Gaussian white noise channel [10]. We assume that the orthogonal sub-channels created through MIMO are dedicated to the same user, and so, the achievable data rate is

$$C = \sum_{i=1}^{min(n_T,n_R)} w\log_2(1+\lambda_i P_i) \tag{4}$$

where P_i is power allocated in ith orthogonal sub-channel, $\sum P_i = P_T$ (P_T is the total transmit power.) and λ_i is the ith orthogonal sub-channel gain, which is obtained through a singular value decomposition (SVD) process as follows.

$$\mathbf{H}^H\mathbf{R}^{-1}\mathbf{H} = \mathbf{U}\Lambda\mathbf{U}^H \tag{5}$$

Here, $\Lambda = diag(\lambda_1, \ldots \lambda_{n_R})$ are the singular values of $\mathbf{H}^H\mathbf{R}^{-1}\mathbf{H}$ and $\mathbf{U}$ is a unitary matrix consisting of the eigenvectors of $\mathbf{H}^H\mathbf{R}^{-1}\mathbf{H}$. Note that, when we compute the singular values, large-scale fading (distance, path-loss, ζ) scales them in *both the interfering MIMO channel matrix and the desired MIMO channel matrix for a given SP's receiver*.

The transmit power allocation for each antenna can be determined in different fashions. The optimal strategy that maximizes capacity [8,9] is the classic water-filling algorithm. However, it requires comprehensive channel information to be known by both the transmitter and the receiver.

$$C = \sum_{i=1}^{min(n_T,n_R)} w\log_2(1+p_i\lambda_i) \tag{6}$$

where p_i is the power allocated to the ith orthogonal sub-channel and $\sum p_i = P_T$ [5].

[4] It is possible that the applications and devices may be very different, some using SISO and others using MIMO. We assume MIMO with both SPs for simplicity.

[5] The optimal transmit signal covariance matrix is $\Sigma_s = (N_0/2)\mathbf{U}diag(p_1, \ldots, p_{n_R})\mathbf{U}^H$ where $p_i = (\mu - \frac{1}{\lambda_i})^+$ and μ is chosen such that $\sum_{i=1}^{min(n_T,n_R)} p_i = P_T$. The function $(.)^+$ denotes the larger one of . and 0.

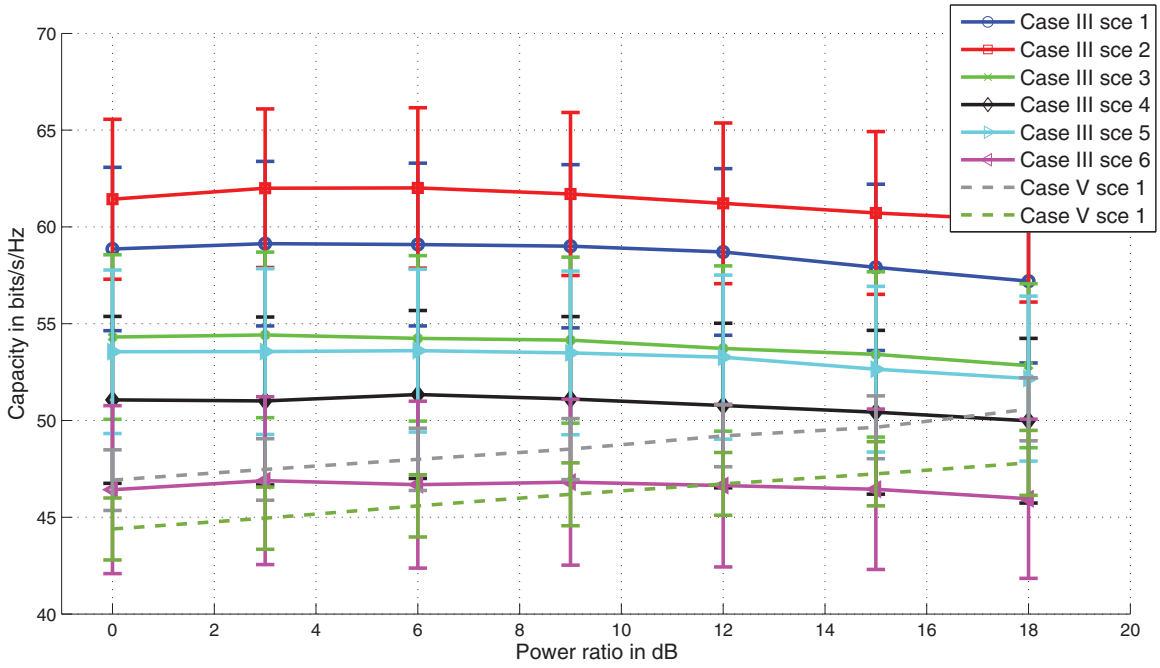

Fig. 6. Aggregate spectral efficiency of the multi-cell system.

We use as one of our metrics, the area aggregate spectral efficiency,[6]

$$\eta = \frac{C_A + C_B}{w_{tot}} \tag{7}$$

where C_A and C_B are the achievable data rates (capacity) in SP_A's and SP_B's layouts, respectively. They are the sum of the achievable data rates of *all the MUs* subscribed to SP_A and SP_B within the coverage. That is, $C_A = \sum_{i=1}^{nu_A} C_i$ and $C_B = \sum_{j=1}^{nu_B} C_j$, where C_i and C_j are calculated by Eq. (6).

3. Simulation results

Simulations to analyze the five cases are based on a multi-cell FFR virtual system, as shown in Fig. 4. MUs in the SP_A layout are distributed uniformly over the radius of the gray area ($2r_A$) and the angle (2π). The distances between a MU and BSs of Cell 1, 2 and 3 and the corresponding receive powers Pr_{A1}, Pr_{A2} and Pr_{A3} are calculated. SP_A decides which cell any given MU is associated with according to the strongest RSS from BS's 1, 2, and 3. If none of the received powers at the MU is larger than $P_{th_A} = P_A r_A^{-\alpha}$ (P_A is transmit power of BSs 1 to 3), we assume this MU is not supported in SP_A's layout. Around 20% MUs are dropped from the simulation with this assumption. In SP_B's layout, we distribute MUs uniformly over the radius of the small cell (r_B) and the angle (2π), and no further cell-selection process is used. Results shown are averages of 10,000 simulation runs that vary locations, ζ, and h_{ij}. The complex channel matrix (for either the transmission from the intended transmitter or interference from any interfering transmitter) is generated using Eq. (1) as described in Section 2.3. The path-loss exponent α takes the value of 4 and $\zeta = N(0, \sigma)$ where $\sigma = 8$.[7] We assume that $w_A = 10$ MHz and $w_B = 5$ MHz and so, the total bandwidth $w_{tot} = 15$ MHz. At each BS, $n_T = 4$ antennas and at each MU, $n_R = 2$ antennas are assumed unless otherwise discussed. The transmit power $P_B = 1$ W is the transmit power of BS-4. BSs 1, 2, and 3 have a power $P_A = P_B \times$ Power Ratio where the power ratio scales the transmit power P_A compared to P_B. The value of $N_0 = -174$ dBm/Hz [13]. Unless specified, the FFR spectrum assignments are $bp_c = \frac{32}{50}$ and $bp_e = \frac{18}{50}$, which means $f_0 = \frac{32}{50} w_A$, $f_1 = f_2 = f_3 = \frac{6}{50} w_A$ ($w_A = 10$ MHz). If the received power at a MU is no larger than $2P_{th_A}$ (3 dB higher than P_{th_A}), it is defined as a cell edge MU in SP_A's layout.

3.1. General trends

We first examine the general trends using Case III and Case V. We pick these cases as our primary objective is to look at configurations that employ FFR and either use virtualized radio resources or perform orthogonal spectrum sharing. In subsequent sections, we consider all five cases. Since results will depend on transmit powers and other parameters, we set up six scenarios, summarized in Table 2. The radius $r_A = 1000$ m. The first three scenarios in Table 2 have a small radius ($r_B = 50$ m) for BS-4 while scenarios 4–6 use a radius of $r_B = 100$ m for BS-4. Also, we consider that BS-4 is at different distances $d = 500, 800, 300$ m from BS-2 (see Fig. 4). However, the separation distance d does not matter when separate/orthogonal spectrum sharing (Case V) is used. This is different from any other case since Case V is the only case in which no sharing happens between SPs. Hence, we list two scenarios for Case V in Table 2 separately. In each scenario, there are almost 300 MUs subscribed to SP_A (100 per base station, but around 20% of the MUs at the edge of the gray circle in Fig. 4 are dropped) and 10 MUs subscribed to SP_B.

The aggregate spectral efficiency in Eq. (7) is determined from simulations for the scenarios described in Table 2 and shown in Fig. 6. The x-axis in this figure corresponds to the ratio P_A/P_B. Error bars correspond to one standard deviation of the mean over 10,000 runs. The variation in capacity results primarily due to the varying locations of MUs (and also due to the random fading). We see that the aggregate spectral efficiency in Case III is better than that in Case V for most of the scenarios. This gain comes exclusively from RRV (simultaneous use of interfering spectrum) indicating that it is possible to exploit RRV for better spectrum usage than using orthogonal-only slices with SSV that has been considered in the most of the existing work on

[6] The area spectral efficiency of a cellular system is defined as the achievable data rate per unit area for the bandwidth available. Here we assume the area of SP_A's layout to be the unit of area of interest, so the measure of area spectral efficiency is in terms of bit/s/Hz/(area of SP_A's layout) [11,12].

[7] We generate h_{ij} as a complex Gaussian random variable, $\sqrt{\frac{1}{2}}(a + j * b)$ where a and b are independent and $N(0, 1)$, once for each run.

Table 2
Parameter settings for various scenarios.

ID	Radius of BS-4	Distance *d* of BS-4 from BS-2		Remarks
1	50m	500m	Case III	BS-4 has small radius, is at different distances from BS-2
2	50m	800m		
3	50m	300m		
4	100m	500m		BS-4 has larger radius, is at different distances from BS-2
5	100m	800m		
6	100m	300m		
SSV 1	50m	-	Case V	BS-4 has two different radii, MUs have better channel in smaller cell
SSV 2	100m	-		

wireless virtual networks. Fig. 6 also provides some insights that are not obvious, assuming that aggregate spectral efficiency is the metric of interest.

- RRV with FFR is *not necessarily* the best option always. However it is better than FFR/SSV in several scenarios.
- Increasing the power ratio (P_A/P_B) from 0 to 18 dB changes the average aggregate spectral efficiency minimally (it is essentially flat).

The reason for the second observation is that the distances from BSs 1, 2, and 3 to SP_A's MUs are large and increasing the power ratio does not a result in a very significant change in the capacity. On the contrary, the separation distance d and cell radius r_B are influential. However, the way in which they impact capacity are different for SP_A and SP_B's MUs which will be discussed next.

While aggregate capacity is useful, how the cases and scenarios would affect the capacity of each SP is important. This would determine the configuration that is provided by the resource manager in Fig. 1. The average achievable data rate for each MU in SP_A's and SP_B's layouts are shown in Fig. 7 for all the scenarios in Table 2. The per MU data rate in SP_A's layout clusters together and appears to be mostly independent of the scenario. Further, sharing of spectrum provides limited gains since MUs of each SP share the available bandwidth orthogonally. So, the extra available bandwidth for SP_A's MUs is not significant since SP_A's layout has almost 300 MUs. When the power ratio is lower than 9 dB or so (this ratio varies slightly across scenarios), the capacity for MUs in SP_A's layout with Case III is worse than with Case V. Therefore, it may be necessary for the resource manager to carefully consider the options to ensure sufficient capacity for MUs in SP_A's layout.

In SP_B's layout, as only 10 MUs share the entire available bandwidth (at least 5 MHz) the achievable data rate is much higher than it in SP_A's layout – also the path loss is much smaller in BS-4 due to its size. Further, for most scenarios, the achievable data rate in SP_B's layout is higher with Case III than with Case V. The capacity in SP_B's layout substantially increases due to the extra spectrum that MUs subscribed to SP_B get through RRV and it is the main contributor to the increase in aggregate capacity. The capacity increases with the separation distance d, but reduces when the small cell's radius r_B increases, i.e., they both impact the capacity. For instance, Scenarios 3 and 5 from Table 2 have very similar capacity values, although the numbers are not identical. In Scenario 3, the cell radius $r_B = 50$ m is small, but the separation distance $d = 300$ m is also small. In Scenario 5, the cell radius $r_B = 100$ m is large, but the separation distance $d = 800$ m is also large. When r_B is small, MUs are closer to BS-4 and the interference from BS's 1,2, and 3 is small compared to the desired received power. When r_B is large, the desired received power is smaller, and the interference may be larger for some MUs. This interference can be made smaller if the separation distance is large, i.e., the MUs of SP_B are much farther away from the major interfering BS (BS-2). We also note here that d is the distance between BS-2 and BS-4 (see Fig. 4). We keep it less than r_A in our simulations (which means the BS-4 is within BS-2's coverage). The performance would be similar when d is larger than r_A (BS-4 would move into BS-1, but the impact is the same).

3.2. Comparison of cases

Next, we consider a comparison of the various cases described in the previous section, with the six scenarios in Table 2 to get some insights into how a resource manager may pick configuration options.

Figs. 8 and 9 provide the comparisons of the various cases for two power ratios (P_A/P_B) of 3 dB and 15 dB. In the former, the larger cells (BS-1, 2, and 3) operate at a power that is only 3 dB higher than BS-4, while in the latter, this value is 15 dB. From Fig. 7, we see that FFR/SSV (Case V) may be better for SP_A's layout when the power ratio is 3 , but not if the power ratio is 15 dB. In these figures, we only plot the *average capacity per MU* and do not show the variability to avoid clutter. There is variability across cases and scenarios as shown in Fig. 7. In each figure, the top graph shows the results for MUs in SP_A's layout while the bottom shows the results for MU's in SP_B's layout. We make the following observations from these plots.

- The scenario (size of BS-4's cell or its distance d from BS-2) does not impact the capacity per MU for MU's in SP_A's layout in a perceptible way. However, the cases (how spectrum is shared) matter substantially. This is NOT the case for MUs in SP_B's layout.
- The power ratio P_A/P_B is an important factor, that can change the capacities for the MUs (though it is not as important to change the aggregate spectral efficiency). The power ratio is disproportional between the MUs subscribed to SP_A and SP_B. The capacity of MUs subscribed to SP_B can go up from 30–50 Mbps (when the power ratio is 15 dB) to 30–60 Mbps (when the power ratio in 3 dB). On the contrary, MUs in SP_A's layout see a decrease from a maximum of 2.3 Mbps to 1.8 Mbps respectively.

Please cite this article as: X. Wang et al., On configuring radio resources in virtualized fractional frequency reuse cellular networks, Computer Communications (2015), http://dx.doi.org/10.1016/j.comcom.2015.10.013

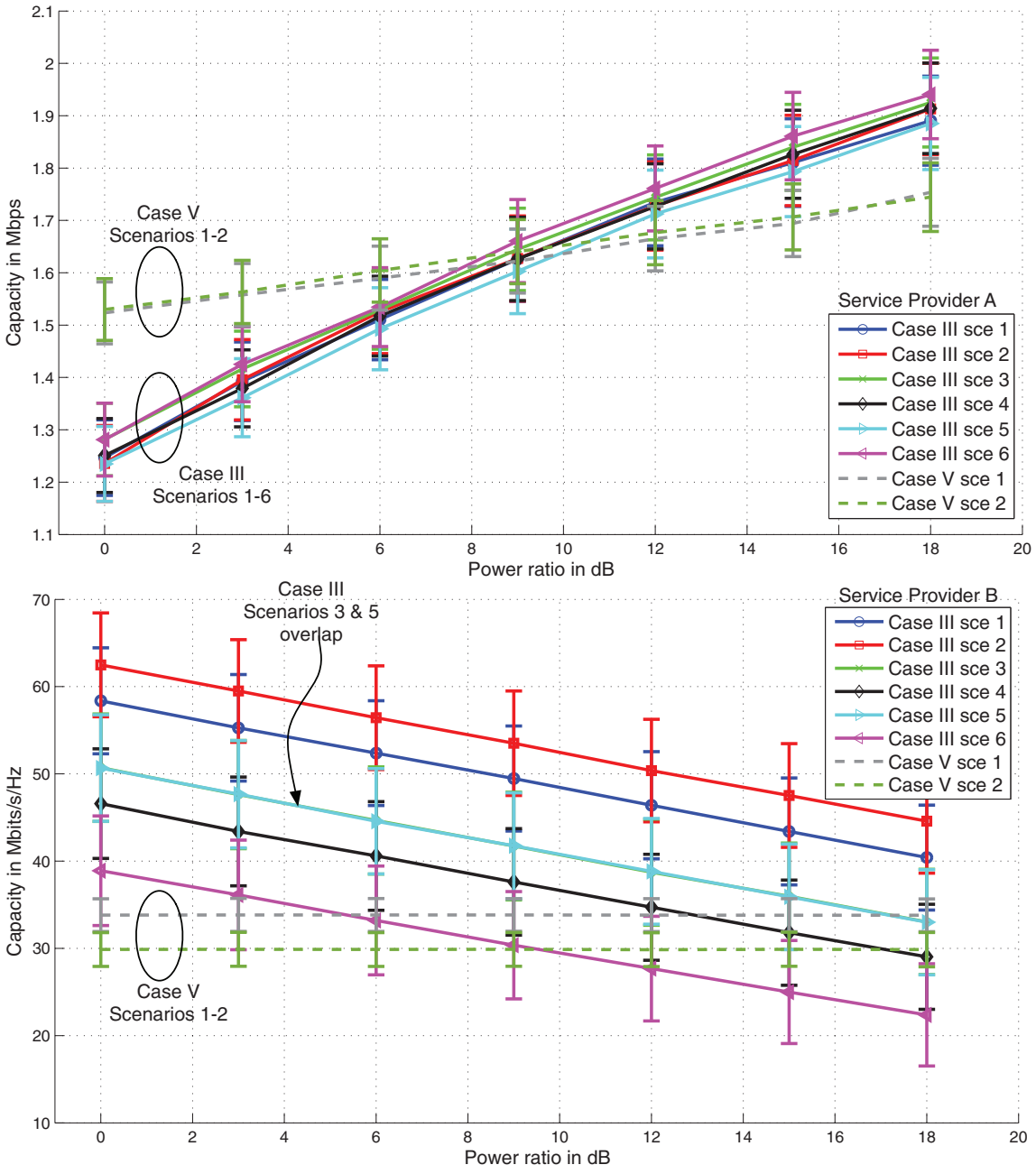

Fig. 7. Achievable data rate (per MU) – top (SP_A's layout) and bottom (SP_B's layout).

- The best strategy for configuring spectrum resources for MUs in SP_A's layout is not the best strategy for MUs in SP_B's layout and vice versa. For instance, Case IV (Center + FFR + RRV) is the best spectrum configuration for MUs in SP_A's layout in all scenarios. However, Case I (RRV), Case II (Freq. reuse + RRV) and Case III (FFR + RRV) behave comparably for MUs in SP_B's layout. In fact, for the MUs in BS-4, it does not matter (on average) much how the spectrum is configured for use by MUs in SP_A's layout as long as all of the spectrum is configured for use by them. They are affected only in Cases IV and V when their share of spectrum is reduced.

To understand the results better, we plot the average capacity per MU in SP_B's layout versus the average capacity per MU in SP_A's layout for the various cases, scenarios and power ratios of 3 dB and 15 dB in Fig. 10. Ideally, we would like to see results in the top right corner of these plots. That is, MU's in both SP_A's layout and SP_B's layout see high capacity, but clearly, that is not feasible for all scenarios and cases. However, the average capacities show some interesting trends that can be used from a resource manager's perspective towards configuring a virtual network based on the SPs' requirements (capacities).

- The influence of the power ratio is clearer in Fig. 10. When the power ratio increases from 3 dB to 15 dB, SP_A's capacities are higher while SP_B's capacities are lower (the average capacity points shift toward the lower right corner).
- The average capacities follow similar patterns if the power ratios P_A/P_B of 3 dB and 15 dB are considered separately. For SP_A, scenarios belong to the same case do not see varying average capacities (capacity points for a given case – e.g., RRV + FFR – but different scenarios align almost vertically). However, the average capacity varies across cases (vertical lines are separated and occur at different capacities for MUs of SP_A). For the MUs of SP_B, the average

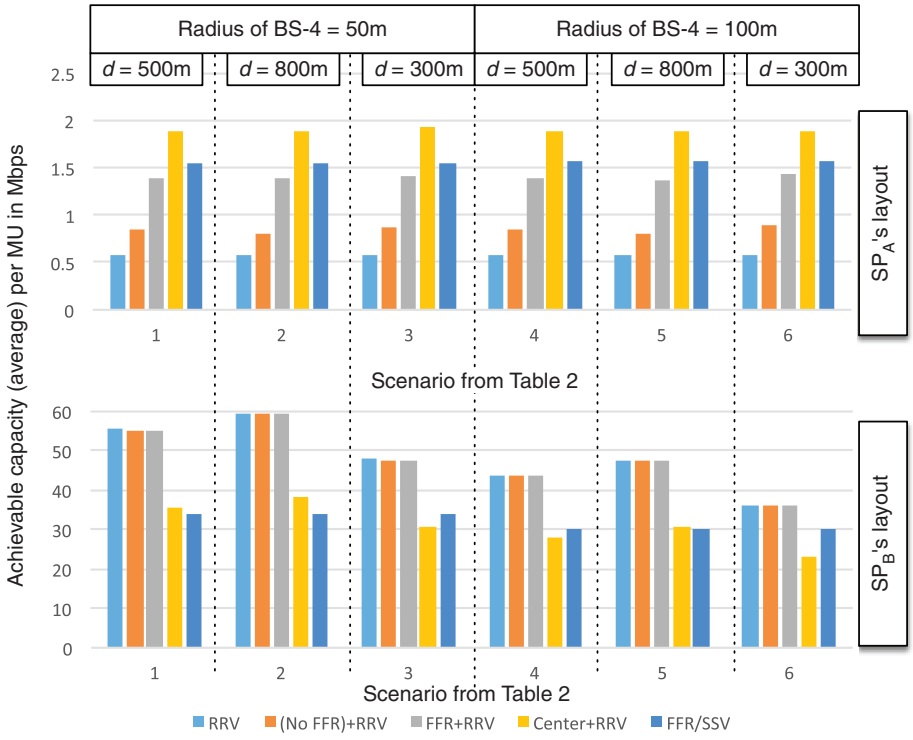

Fig. 8. Comparison of achievable data rate per MU in SP_A and SP_B's layouts for a power ratio of 3 dB.

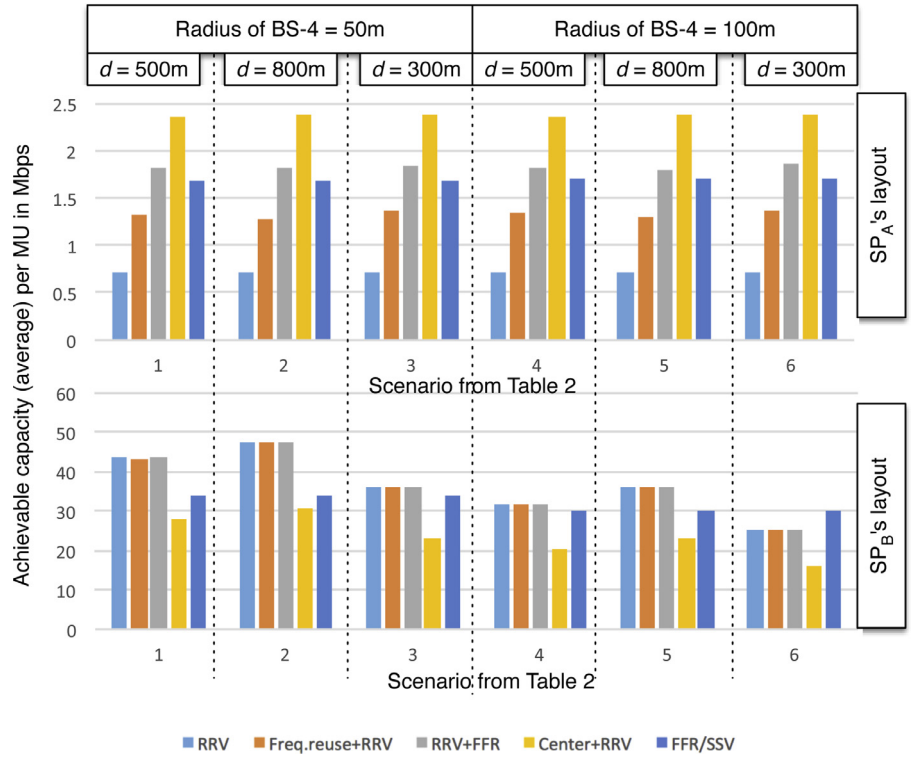

Fig. 9. Comparison of achievable data rate per MU in SP_A and SP_B's layouts for a power ratio of 15 dB.

capacities vary across both cases and scenarios. Scenario 2 with small r_B and large d is the best in every case for SP_B. Cases in which SP_B can share all of the radio resources (Cases I, II and III) are most beneficial.

- We can say that if SP_A's demand is the resource manager's primary concern, the preferred configuration options would be Center + FFR + RRV regardless of the scenario. On the other hand, a resource manager trying to increase SP_B's capacity in the hotspot would discard the Center + FFR + RRV and FFR/SSV options.
- FFR + RRV provides the greatest aggregate capacity (most towards the top right corner) and mutual benefits for both SPs. Therefore, it is a desirable configuration, almost always. Orthogonal

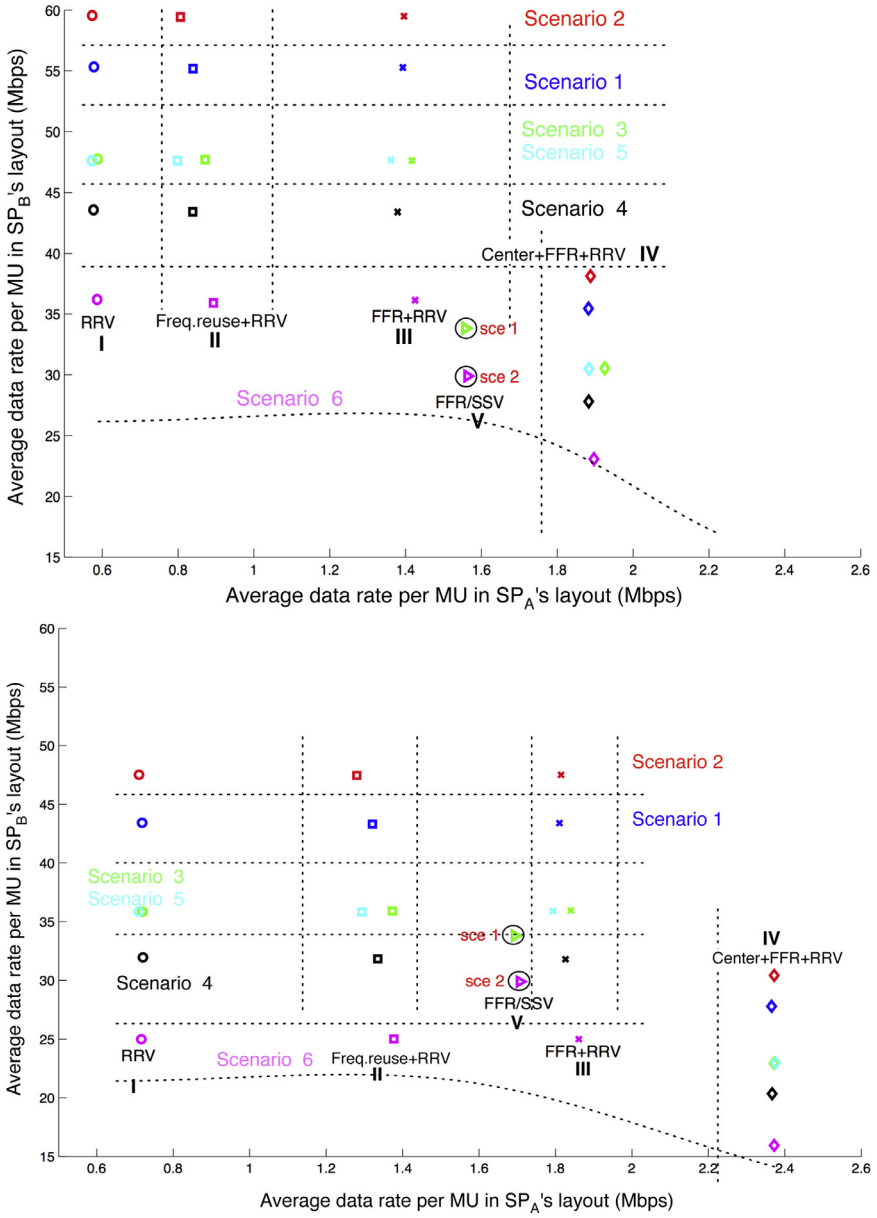

Fig. 10. Capacity in SP_A layout vs. capacity in SP_B layout – top (3 dB) and bottom (15 dB). (For interpretation of the references to color in this figure legend, the reader is referred to the web version of this article.)

spectrum sharing through FFR/SSV helps SP_A when the power ratio is low (3 dB, as observed previously), but the benefits are only minimally better than the FFR + RRV case. Especially when SP_A is able to transmit at a relatively high power level, FFR + RRV is the best option.

3.3. Configuration map

We can view Fig. 10 as a *configuration map* for use by the resource manager. We have drawn dotted lines to separate various cases and scenarios – this splits the figures into a tabular format where every point can represent the demands of the two SPs and includes tradeoffs between them.

We redraw this configuration map for clarity in Fig. 11. The associated scenario and case show the network environment and configuration. A resource manager could choose or switch between configurations to adjust the sharing according to the SPs' requirements. We explain this through two simple examples:

- (a) Let us suppose that in a given time unit, the network environment is similar to scenario 1 (blue dots in Fig, 10 or blue area in Fig. 11). SP_A reports that its required capacity is no less than 1.8 Mbps and SP_B has a demand in the hotspot that is no less than 35 Mbps per MU. The configuration options are either Case IV: Center + FFR + RRV or Case III: FFR + RRV. With the Center+FFR+RRV option, the power ratio should be 3 dB. However, if the resource manager chooses FFR + RRV, it has to configure SP_A to transmit at least 15dB higher than the power of SP_B in BSs 1, 2, and 3. Note that Center+FFR+RRV shares a smaller slice of the spectrum.
- (b) Suppose the network environment is similar to scenario 2 (red dots in Fig. 10 or red area in Fig. 11). In a given time unit, the capacity demands of SP_A and SP_B are around 2 Mbps and 20 Mbps per MU in their layouts. The configuration applied by the resource manager is Case IV: Center + FFR + RRV with a power ratio of 15 dB. If there is a spike in SP_B's hotspot (BS-4's) demand to 35 Mbps, the resource manager (based on the service agreement) may reconfigure the network in the next time unit to Case III: FFR + RRV

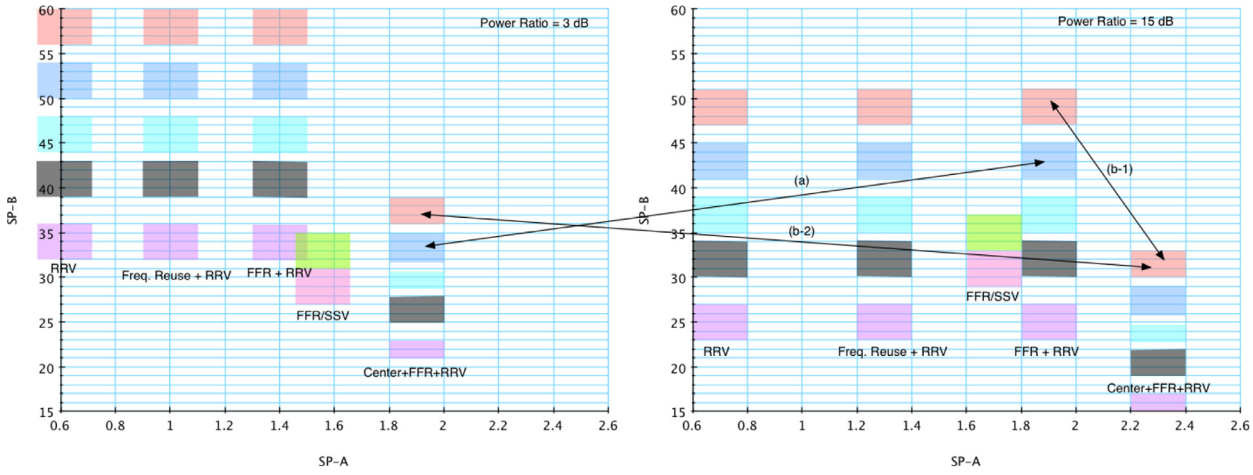

Fig. 11. Using configuration map by resource manager. (For interpretation of the references to color in this figure legend, the reader is referred to the web version of this article.)

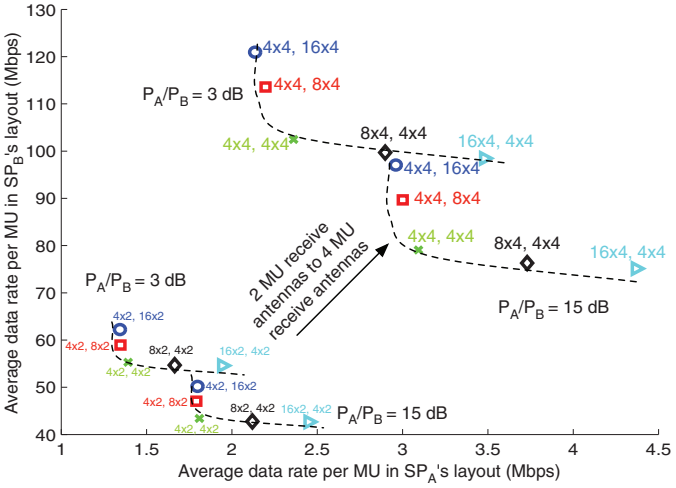

Fig. 12. Capacity in SP_A layout vs. capacity in SP_B layout for various MIMO settings.

reducing the capacity per MU of SP_A to 1.85 Mbps and increasing it to 47 Mbps for SP_B by allocating more spectrum for use by SP_B while increasing the interference to MUs of SP_A. Alternatively, the resource manager could stay with Case IV and reduce the power ratio to 3 dB. We observe that in each case, the cell edge MUs in SP_A's layout are likely to be impacted negatively.

3.4. Impact of number of antennas

MIMO settings as an important part of configuration has a major influence on system and per MU achievable capacity. We assume all sub-channels created through MIMO are dedicated to the same MU (Eqs. (4)–(6)), hence capacity proportionally increases as the number of sub-channels ($min(n_T, n_R)$) [6]. Due to hardware limits, it may not be practical to implement more than 2 antennas at the MUs. However, we do consider 2 and 4 antennas at the MU while changing the number of antennas at BSs 1, 2, 3, together and BS-4 to examine the ability of MIMO in combating interference. We use scenario 1 of case III as representative and plot the average capacities in Fig. 12. In this figure, a pair of products $x \times y$, $p \times q$ indicates the number of BS transmit antennas $\times$ the number of MU antennas of SP_A and SP_B respectively. We observe the following:

- The trend of capacities of MUs of SP_A and MUs of SP_B for the power ratios of 3 dB is the same as the trend for 15dB. In the two upper curves, when the number of SP_A's antennas is fixed (e.g., 4), as the number of antennas used at SP_B's BS-4 is doubled, the average capacity per MU for SP_B increases by 7–10 Mpbs (around 7%). The capacity per MU of SP_A drops only slightly even though more antennas are transmitting in BS-4. A similar result is observed when SP_B uses a fixed number (e.g., 4 antennas) while SP_A doubles the number of antennas. For example, when the power ratio is 3 dB, the average capacities for MUs of SP_B barely change but the capacity for MUs of SP_A increase from 2.35 Mbps to 3.5 Mbps after the number of antennas is quadrupled. This may be a configuration strategy that can be adopted by a resource manager to quickly improve a SPs' capacity.
- If device heterogeneity can be exploited (which is a possibility in the future), we see that the curves can be moved towards the right top corner in Fig. 12 by configuring the system differently with increasing numbers of mobile antennas.

4. Discussion

In this section, we discuss some outstanding issues partially. Further study is required to understand these issues in the context of radio resource virtualization.

4.1. Isolation

One of the challenges of virtualization is the isolation of users (in this case SPs) from each other. The use of a resource by one SP should not adversely impact a second SP.

In Figs. 8–10, we have only shown the average values of the capacity for MUs over several simulation runs. While the averages provide a good indication of the long term capacities, there is appreciable variability around this mean value over smaller time units. Fig. 13 shows the variation for two cases (Cases III and IV), both Scenario 1, for power ratios of 3 dB and 15 dB. The plot only includes 100 runs to avoid clutter and the average values reflect this, compared to the 10,000 runs in the previous results. Clearly, the variability has impact on the achievable data rates for MUs of the two SPs due to the varying locations of MUs and the varying channel conditions. The resource manager and InPs may be able to use data to provide *probabilistic service agreements* that provide average capacity values with certain probabilities. The variability alerts us to be aware of the fact that misconfigurations of one or both SPs will have considerable impact on the isolation between them. If SPs are allowed to configure the hardware with the parameters supplied by a resource manager, and they behave selfishly or maliciously, the impact may be worse.

The challenges of isolation between SPs needs substantial thought and it is part of our ongoing work.

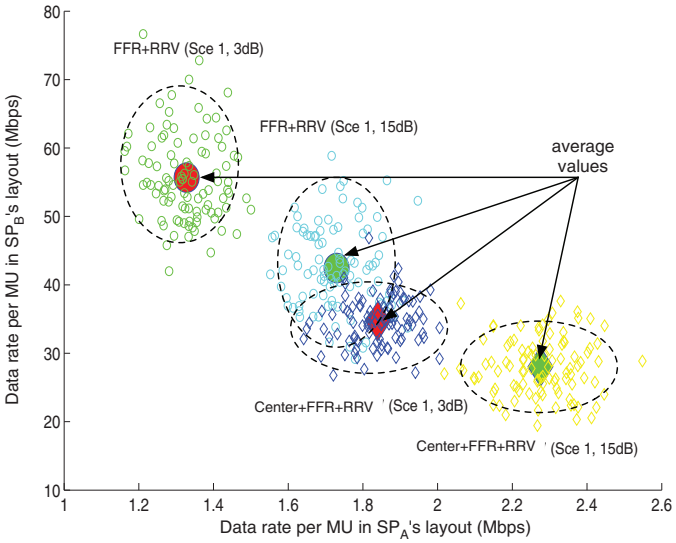

Fig. 13. Variation in capacity.

Table 3
Percentages of cell edge MUs.

Cell edge range	1 dB	2 dB	3 dB	4 dB	5 dB	6 dB
Percentage	0.043	0.091	0.141	0.194	0.248	0.304

4.2. Impact on cell-edge users due to FFR in SP_A's layout

There are two factors that impact the capacity of cell edge MUs - how much spectrum is allocated to them and how we define the cell edge. The cell edge is defined by a dB value that is larger than P_{th_A}. The average fraction of cell edge MUs at varying cell-edge ranges are listed in Table 3. The fewer the cell edge MUs, the more spectrum they have (since the spectrum is partitioned in a deterministic manner). We examine Case III, Scenario 1 here.[8] The transmit power ratio is 10 dB.

Fig. 14 shows the average achievable data rates over *all MUs* and over only *cell edge MUs*. As more spectrum ($82\% = \frac{41}{50}$) is allocated to center MUs, the overall capacity (achievable data rate per MU) has a mild improvement. At the same time, the average data rate per cell edge MU drops. The cell edge capacity per MU drastically falls with the increasing edge area because more MUs share a limited spectrum. On the contrary, the overall average data rate does not change much even when the cell center area shrinks. Note that here we provide 3 cases of partitions with changeable edge area to give an impression of the interaction between those parameters. The optimal partition in virtual FFR system requires more detailed evaluation metrics like user satisfaction [14]. We used a 3 dB threshold in our simulations since the cell edge MUs have almost the same capacity as the overall MUs in each cell when $64\% = \frac{32}{50}$ of spectrum is allocated to center MUs.

4.3. Other issues and future work

For simplicity, the system model in this paper assumes the transmit powers are the same in all spectrum slices allocated to a given SP. If a snapshot is taken, the BSs transmit to MUs of the same group (e.g., SP_A center MUs, SP_A cell edge MUs, and SP_B MUs) at the same power level. This need not be the case and the powers may be tuned to different MUs. The other assumption made here is that the orthogonally-divided frequency slices for one SP are distributed randomly to its MUs. In reality, this might not be the best case. The interference level and channel conditions in different frequency slices may be different. Cells 1, 2 and 3 may operate at different transmit power levels. As a result of these differences, the interference seen by SP_B's MUs may be different. Further, different definitions of cell edge are possible in Cells 1, 2 and 3.

The consequence of these changes is that units of spectrum assigned to MUs could be differentiated by interference levels. The tradeoff of capacities will boil down to the MU level instead of a SP level. For instance, every slice of spectrum may have a particular Receive Signal Strength (RSS) level which indicates the power level that another transmission can apply at the same time. The resource manager will have to configure concurrent transmissions in a given spectrum slice based on the MUs' required capacities. Moreover, power control scheme and interference coordination need to be considered in such heterogeneous architecture. Eventually the configuration problem addressed in this paper will cope with other strategies. A global optimality would be achieved through formulating a problem taking configuration, power allocation, interference coordination and cost into account. Some existing global optimization problems are presented in [15–17]. [15] designed a problem that optimizes inter-BS scheduling considering interference hence minimize the content transmission time. [16] and [17] focus on power-control schemes in the generalized problems. The former mitigates interference by multi-channel power allocation while the later wisely adds penalty to power-consumption to maximize the net utility (defined as utility minus cost).

Since MIMO has been considered, we assume the number of antennas set by every pair of transmitter and receiver can vary to meet the request of a service. There is limit at user devices and it could be a constraint when a SP evaluate its overall network performance. Scheduling based on channel quality (e.g., the proportional fair (PF) scheduler in LTE [18]) also may impact capacity. With channel quality information of MUs in every time unit, the system schedules radio resources to MUs which have good channel conditions. It may be possible to group MUs to achieve pareto optimality as described in [19]. Our future work will be along this line to deploy more flexible configurations to facilitate efficient radio resource virtualization.

5. Related work

We interpret wireless virtualization as a derivative of wired virtualization. In fact, some network entities in the radio access network (RAN) architecture have already been virtualized, driven by wireless resources sharing. In this section, we briefly introduce work similar and related to wireless virtualization. We also describe some key technologies adopted in our system.

In wireless networks, mobile network operators (MNOs) have controlled resources for decades. They are often involved in selling the end-devices to subscribers, building the RAN through which subscribers are connected to the backhaul network, and own and operate the backhaul network as well. Such highly integrated architecture does not differentiate between who provides services and who owns and operates the infrastructure (hardware/software/radio). With the drastic growth in demand for wireless data services, such a structure can become an obstacle against innovation and competition. Wireless network virtualization can be viewed as an alternative architecture of cellular networks which creates a more flexible environment for resource management that improves resource usage and facilitates innovation. In one form of virtualization, the functions of a conventional mobile network operator are decoupled and distributed to two new entities – a SP and an InP. The former is in charge of end-to-end services and the latter is only responsible for maintaining/operating physical resources (RAN, core network, backhaul, and spectrum). This new architecture facilitates resource sharing which is a solution to

[8] We also examined the overall and cell edge performance for other scenarios. The results are neglected here since the high similarity to Fig. 14.

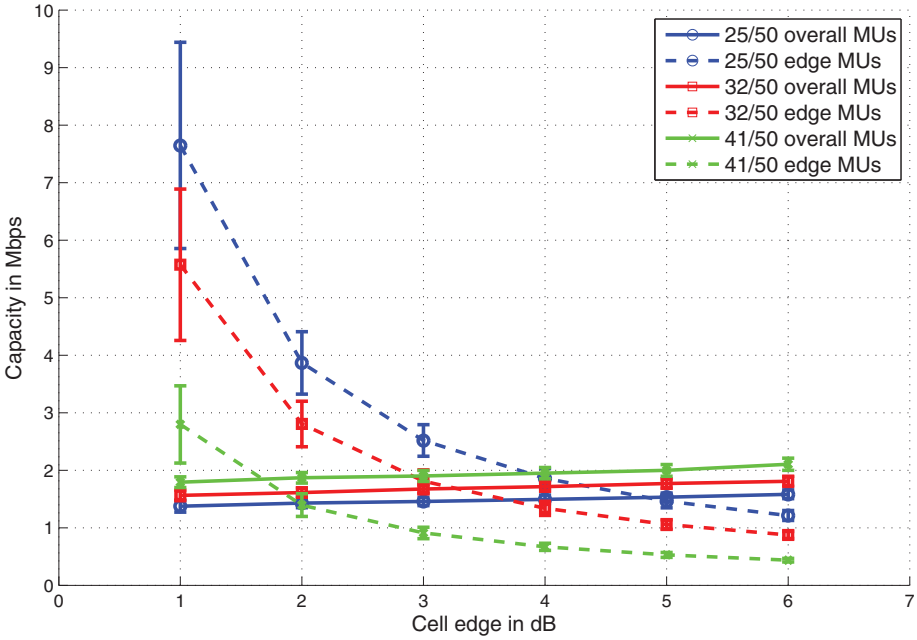

Fig. 14. Achievable data rate per MU for cell center MUs and cell edge MUs.

the scarce spectrum problem in wireless networks. An extreme form of wireless virtualization includes infrastructure virtualization and spectrum virtualization. Note here that the infrastructure refers to all other physical resources except spectrum (e.g., base stations, mobility management entities, serving gateways, etc.).

The idea of virtualization first appeared in wired networks and cloud computing [20]. In wired network virtualization, InPs logically partition a physical network into virtual networks that consist of virtual routers, switches, cross-connects, virtual links, and bandwidth on each link [2]. The virtual elements are usually part of the physical ones and configured based on the agreements SPs have made with InPs. Such virtual networks then are assigned to SPs on demand. Multiple SPs may operate their virtual networks on top of the same physical substrate without knowing the underlying infrastructure. This service model, in the case of wireless networks, is similar to existing MVNOs which provide services through network resources leased from multiple MNOs [21]. However, an MVNO does not enable a sharing of the RANs among MNOs. The common situation is that an MVNO uses a single MNO. Once the agreement is built out, resources in the RAN and in the backhaul are leased exclusively to a certain MVNO on a long term.

Unlike MVNOs, *wireless virtualization allows sharing to occur in fine-grained manner*. The partition of either spectrum or other physical resources is fluid according to temporal demands of different SPs. Dynamic spectrum access (DSA) views wireless virtualization as a new spectrum sharing model in which spectrum is auctioned as a continuous good as opposed to a discrete item [21]. Recently, wireless virtualization is being examined not only from an economic perspective, but improvements in system capacity and technical feasibility have also been studied in specified networks (WiMAX, LTE, etc. [4,5,7]). A complete sharing in wireless networks can fully exploit the available resources, but also induces challenges and issues. Since transmissions in wireless networks go through air interfaces, virtualization may cause fierce interference among the transmissions of SPs without a coordinated configuration which is the focus of this paper.

The 2-SP network structure considered in this paper is similar to a typical heterogeneous network (HetNet) where small cells are distributed in the macrocell to enhance coverage and offer users larger bandwidth. HetNet deployment aims at achieving "offloading gain" that alleviates the load on a macrocell's crowded spectrum. The objective of a virtualized network (as in this paper) is not to offload users from one SP to another, but to *make wireless networks a flexible environment that accommodates diverse SPs and provides reliable services for each SP*. Note that HetNets are operated by the same MNO that owns the network infrastructure and spectrum. In HetNet deployment, the cross-tier signal-to-interference plus noise ratio (SINR) is evaluated to guarantee reliable coverage in each tier [11,12]. Indoor Femtocells sometimes naturally provide interference separation (due to building walls, etc.) ensuring the quality of indoor transmissions without interfering with the users in the outdoor cells. Outdoor HetNets either coordinate concurrent transmissions of macrocell and small cells to avoid severe interference or operate them in separate bandwidths. Such coordination is possible because one operator controls both macrocells and small cells. However, our work not only focuses on the overall system capacity improvement but also the balance of capacity tradeoffs between SPs sharing the same radio resources. Also, unlike a single-operator HetNet, layouts in the virtual network in this paper are used by different SPs. Coordinated transmissions, if any, have to be facilitated by a resource manager making it more complicated. Though the idea of virtualization is completely different from HetNet, some insights from this paper might be applied in HetNets also.

Recently, software defined networks (SDNs) [22] have been considered with wireless virtualization in the context of next generation wireless networks/5G networks [23]. As a concept extended from wired virtualization, SDN is considered as a promising network architecture because of its centralized traffic-control function. In SDNs, the data plane and control plane are separated and wireless devices only forward data traffic. A global central controller is in charge of network management, including configuring network settings and to guarantee quality of services (QoSs) [24]. From a functionality perspective, the framework described in this paper could be used by a central controller, in some ways smoothly merging wireless radio virtualization with SDNs.

FFR and MIMO are considered as interference mitigation strategies. FFR was originally proposed by Halpern [25] to manage intercell interference. FFR schemes partition the total frequency band into multiple parts. Some parts are used in the center area of every cell

Please cite this article as: X. Wang et al., On configuring radio resources in virtualized fractional frequency reuse cellular networks, Computer Communications (2015), http://dx.doi.org/10.1016/j.comcom.2015.10.013

while the others are reserved for use at cell edges. Users with good reception conditions may access bands with low reuse factor (i.e., reuse factor= 1). Users with bad reception conditions (at the edges) access bands with high reuse factor (e.g., reuse factor= 3). FFR increases system-wide spectral efficiency without loss in cell edge performance. Based on the same idea of cell wise usage restrictions, Gerlach et al. invented an "inverted" FFR that further improved spectral efficiency and optimized frequency planning in a self-organized way [26]. The work in [27] implemented heterogeneous elements on top of the macrocell FFR layout and demonstrated gains in throughput and reliable coverage. In this paper, in addition to deploying spectrum sharing, we also test the ability of FFR to increase spectral efficiency (compare Cases I, II, and III) for SP_A. Further, we include the benefits of MIMO with the virtual settings and use MIMO channel capacity as the capacity evaluation metric. This information theoretic metric was proposed in [8] to evaluate the capacity of a MIMO channel with interference using a combined SINR matrix. Multiuser detection methods for combating inter-cell interference have been developed and evaluated using this matrix [9]. The outage capacity of MIMO channels under different types of interference has also been calculated [28].

6. Conclusions

In this paper, we use simulations to examine the problem of radio resource configuration when wireless networks are virtualized. We evaluate several scenarios with several spectrum sharing cases that include FFR. The paper provides a framework for a resource manager to configure radio resources between two different SPs operating in the same geographical area. The configuration of a virtualized wireless network is unlikely to have a definite "closed form" single solution. Proper configuration depends on the network architecture, capabilities of the network/end-devices and demands of the players, and it changes dynamically. Reasonable configurations appear to be capable of leading virtualization towards higher efficiencies, better isolation across SPs, and customization of services. Configurations investigated are references for future cellular networks with similar advanced technologies.

References

[1] X. Costa-Perez, J. Swetina, T. Guo, R. Mahindra, S. Rangarajan, Radio access network virtualization for future mobile carrier networks, IEEE Commun. Mag. 51 (7) (2013).
[2] X. Wang, P. Krishnamurthy, D. Tipper, Wireless network virtualization, in: Proceedings of the 2013 International Conference on Computing, Networking and Communications (ICNC), IEEE, 2013, pp. 818–822.
[3] H. Lee, S. Vahid, K. Moessner, A survey of radio resource management for spectrum aggregation in LTE-advanced, Communications Surveys & Tutorials. IEEE 16 (2) (2014) 745–760.
[4] Y. Zaki, L. Zhao, C. Goerg, A. Timm-Giel, LTE mobile network virtualization, Mob. Netw. Appl. 16 (4) (2011) 424–432.
[5] L. Zhao, M. Li, Y. Zaki, A. Timm-Giel, C. Görg, LTE virtualization: from theoretical gain to practical solution, in: Proceedings of the 23rd International Teletraffic Congress, 2011, pp. 71–78.
[6] X. Wang, P. Krishnamurthy, D. Tipper, On radio resource sharing in multi-antenna virtualized wireless networks, in: Proceedings of the 16th ACM International Conference on Modeling, Analysis & Simulation of Wireless and Mobile Systems, ACM, 2013, pp. 31–40.
[7] G. Bhanage, I. Seskar, D. Raychaudhuri, A virtualization architecture for mobile WiMAX networks, ACM SIGMOBILE Mob. Comput. Commun. Rev. 15 (4) (2012) 26–37.
[8] R.S. Blum, J.H. Winters, N.R. Sollenberger, On the capacity of cellular systems with MIMO, IEEE Commun. Lett. 6 (6) (2002) 242–244.
[9] H. Dai, A.F. Molisch, H.V. Poor, Downlink capacity of interference-limited MIMO systems with joint detection, IEEE Trans. Wirel. Commun. 3 (2) (2004) 442–453.
[10] D.-s. Shiu, Wireless Communication Using Dual Antenna Arrays, Springer, 2000.
[11] R. Madan, J. Borran, A. Sampath, N. Bhushan, A. Khandekar, T. Ji, Cell association and interference coordination in heterogeneous LTE-A cellular networks, IEEE J. Sel. Areas Commun. 28 (9) (2010) 1479–1489.
[12] Y. Bai, J. Zhou, L. Chen, Hybrid spectrum usage for overlaying LTE macrocell and femtocell, in: Proceedings of IEEE Global Telecommunications Conference, GLOBECOM 2009, IEEE, 2009, pp. 1–6.
[13] 3GPP, TR 36.931 version 9.0.0. Release 9, 2011.
[14] D. Bilios, C. Bouras, V. Kokkinos, A. Papazois, G. Tseliou, Optimization of fractional frequency reuse in long term evolution networks, in: Proceedings of the 2012 IEEE Wireless Communications and Networking Conference (WCNC), IEEE, 2012, pp. 1853–1857.
[15] V. Sciancalepore, V. Mancuso, A. Banchs, S. Zaks, A. Capone, Interference coordination strategies for content update dissemination in LTE-A, in: Proceedings of 2014 IEEE International Conference on INFOCOM, IEEE, 2014, pp. 1797–1805.
[16] K. Son, S. Lee, Y. Yi, S. Chong, Refim: A practical interference management in heterogeneous wireless access networks, IEEE J. Sel. Areas Commun. 29 (6) (2011) 1260–1272.
[17] M. Xiao, N.B. Shroff, E.K. Chong, A utility-based power-control scheme in wireless cellular systems, IEEE/ACM Trans. Netw. 11 (2) (2003) 210–221.
[18] R.B. Marks, et al., IEEE standard 802.16: a technical overview of the WirelessMAN™ air interface for broadband wireless access, IEEE Commun. Mag. (2002) 98.
[19] H. Burchardt, S. Sinanovic, G. Auer, H. Haas, Pareto optimal power control scheduling for OFDMA networks, in: Proceedings of 2012 IEEE Vehicular TechnologyConference (VTC Fall), 2012, pp. 1–5.
[20] N. Chowdhury, R. Boutaba, A survey of network virtualization, Comput. Netw. 54 (5) (2010) 862–876.
[21] T.K. Forde, I. Macaluso, L.E. Doyle, Exclusive sharing & virtualization of the cellular network, in: Proceedings of the 2011 IEEE Symposium on New Frontiers in Dynamic Spectrum Access Networks (DySPAN), IEEE, 2011, pp. 337–348.
[22] D. Kreutz, F.M. Ramos, P. Esteves Verissimo, C. Esteve Rothenberg, S. Azodolmolky, S. Uhlig, Software-defined networking: a comprehensive survey, Proc. IEEE 103 (1) (2015) 14–76.
[23] M.A. Marotta, N. Kaminski, I. Gomez-Miguelez, L.Z. Granville, J. Rochol, L. DaSilva, C.B. Both, Resource sharing in heterogeneous cloud radio access networks, IEEE Wirel. Commun. 22 (3) (2015) 74–83.
[24] B. Cao, F. He, Y. Li, C. Wang, W. Lang, Software defined virtual wireless network: framework and challenges, IEEE Netw. 29 (4) (2015) 6–12.
[25] S.W. Halpern, Reuse partitioning in cellular systems, in: Proceedings of the 33rd IEEE Vehicular Technology Conference, 33, IEEE, 1983, pp. 322–327.
[26] C.G. Gerlach, I. Karla, A. Weber, L. Ewe, H. Bakker, E. Kuehn, A. Rao, ICIC in DL and UL with network distributed and self-organized resource assignment algorithms in LTE, Bell Labs Tech. J. 15 (3) (2010) 43–62.
[27] A. Ghosh, N. Mangalvedhe, R. Ratasuk, B. Mondal, M. Cudak, E. Visotsky, T.A. Thomas, J.G. Andrews, P. Xia, H.S. Jo, et al., Heterogeneous cellular networks: from theory to practice, IEEE Commun. Mag. 50 (6) (2012) 54–64.
[28] Y. Song, S.D. Blostein, MIMO channel capacity in co-channel interference, in: Proceedings of the 21st Biennial Symposium on Communications, 2, 2002, pp. 220–224.

Please cite this article as: X. Wang et al., On configuring radio resources in virtualized fractional frequency reuse cellular networks, Computer Communications (2015), http://dx.doi.org/10.1016/j.comcom.2015.10.013